THE PUBLISHING HOUSE
OF THE ROMANIAN ACADEMY

PROCEEDINGS OF THE ROMANIAN ACADEMY, Series A,
Volume 25, Number 4/2024, pp. 315–324
DOI: 10.59277/PRA-SER.A.25.4.08

PREDICTION OF UNDRAINED SHEAR STRENGTH BASED ON KMR MODEL

Cheng hang ZHANG [1], Mingyue CHEN [2], Bin LUO [3], Pei LI [4]

[1] Sun Yat-sen University, School of Earth Science and Engineering, Zhuhai, Guangdong 519080, China
[2] Hunan University, College of Civil Engineering, Changsha 410082, China
[3] Taiyuan University of Technology, College of Ecology, Shanxi 030024, China
[4] CCTEG Xi'an Research Institute (Group) Co., Ltd., Shaanxi, 710077
Corresponding author: Cheng hang ZHANG, E-mail: zhangchx65@mail2.sysu.edu.cn
Co-authors: Mingyue CHEN, E-mail: mychen@hnu.edu.cn, Bin LUO, E-mail: luobin@tyut.edu.cn
Pei LI, E-mail: lipei@cctegxian.com

Abstract. The accurate prediction of undrained shear strength is of significant importance in areas such as slope stability, earthquake resistance, and pile foundation design. Therefore, enhancing the accuracy of undrained shear strength prediction is crucial. The research results indicate that employing the KMR model can improve the computational accuracy by 4.4% to 18.9%. Furthermore, compared to conventional empirical formulas, the KMR model evidently processes data more rapidly and can predict relevant parameters more accurately. This method provides a new research idea to some extent for addressing the issue of low prediction accuracy of traditional machine learning models for geotechnical parameters.

Keywords: undrained shear strength, KMR model, machine learning.

1. INTRODUCTION

The undrained shear strength, representing the ultimate capacity of soil to resist shear damage under specific stress conditions and undrained conditions, plays a crucial role in ensuring the safety of geotechnical projects, including highway foundations, dams, and high-rise buildings [1, 2]. Therefore, the reliable assessment of undrained shear strength is a vital task in geotechnical engineering design.

Currently, undrained shear strength is primarily determined through a variety of indoor and field tests [3]. Among these, more region-specific methods such as the cross-plate shear test are commonly used in certain areas, particularly in Asia. However, results from indoor tests may be susceptible to inaccuracies due to sampling disturbances, and it has been observed that these results can be significantly lower than those obtained in field tests [4]. Additionally, findings from sampling test experiments are often not easily generalized.

To enhance the accuracy and applicability of obtained results, some researchers have proposed empirical formulas to estimate undrained shear strength based on extensive testing experiments [5–7]. Nevertheless, these empirical formulas often overlook factors such as soil structure, sensitivity, mineralogical aging, and geological genesis. They fail to capture the high-dimensional nonlinear relationships in the data, rendering the calculation methods unable to flexibly adjust parameters based on actual conditions. Consequently, this leads to a lack of stability in predicting results, which may fluctuate between accuracy and inaccuracy.

With the rapid advancement of computer technology, an increasing array of computer technologies has found applications in the geotechnical field. Particularly, machine learning algorithms have demonstrated remarkable efficacy in geotechnical calculations [8, 9]. However, a singular machine learning model often grapples with the challenge of accurately describing the intricate relationship among various geotechnical parameters, resulting in suboptimal model accuracy. Consequently, some scholars have begun to explore computational methods with heightened superiority [10, 11].

In light of these, the study proposes an advanced KMR (KNN-MLP-RF) stacking model for predicting undrained shear strength, aiming to maximize the amalgamation of accuracy and generalization capabilities from individual base models. A comparative analysis of the stacked model's results with those of the base model and empirical formulas indicates a significant enhancement in the prediction accuracy of undrained shear strength. This underscores the model's ability to effectively integrate diverse base models, address drawbacks and limitations inherent in individual models, and ultimately enhance prediction accuracy.

2. MATERIALS AND METHODS

2.1. Materials

This article utilizes data from clay databases in Jiangsu and Zhejiang, comprising a total of 170 samples [12, 13], mainly collected from Quaternary soils. The geological settings of these sites included the abandoned Yellow River floodplain, lagoons, the Yangtze Delta, the Yangtze marine environment, and the Yangtze floodplain. Specifically, we focused on the cohesive soils from these locations. Undisturbed soil samples were collected at 1.0-meter intervals up to a depth of 25 meters using a 76 mm fixed piston sampler. Once extracted, the samples were sealed with wax at both ends to preserve their integrity. The primary method for acquiring the dataset involves on-site testing. The measured parameters selected in this study include cone tip resistance (q_t), side friction resistance (f_s), pore water pressure (u_2), shear wave velocity (V_s), overconsolidation ratio (OCR), sensitivity (S_t), and undrained shear strength (S_u). q_t describes the failure strength of the soil at the in-situ stress and it is therefore commonly related to the undrained shear strength S_u. QT is normalized cone tip resistance. FS is normalized side friction resistance, refers to the resistance encountered by an object, such as a pile or a cone in a cone penetration test (CPT), as it moves through soil. It is a measure of the frictional force between the surface of the object and the surrounding soil, which contributes to the overall resistance during penetration. BQ is the pore pressure parameter. VS is the normalized speed at which shear waves (a type of seismic wave) travel through a material. In geotechnical engineering, it is used to evaluate the stiffness and elastic properties of soils and rocks. OCR is the overconsolidation ratio. SU is the undrained shear strength ratio.

To mitigate the influence of in-situ stresses on the dataset, normalization and dimensionless processing are performed according to formulas (1) to (7) [14]:

$$\mathrm{QT} = (q_t - \sigma_{vo})/\sigma'_{vo} \tag{1}$$

$$\mathrm{FS} = f_s/\sigma'_{vo} \tag{2}$$

$$\mathrm{BQ} = (u_2 - u_0)/(q_t - \sigma_{vo}) \tag{3}$$

$$\mathrm{VS} = V_s\left(\frac{p_a}{\sigma'_{vo}}\right)^{0.25} \tag{4}$$

$$\mathrm{OCR} = \mathrm{OCR} \tag{5}$$

$$\mathrm{ST} = S_t \tag{6}$$

$$\mathrm{SU} = S_u/\sigma'_{vo} \tag{7}$$

where p_a is the reference pressure, set to 100 kPa (standard atmospheric pressure), σ_{vo} is the total vertical stress, σ'_{vo} is the vertical effective stress.

The mean (Mean), standard deviation (σ), maximum value (Max), and minimum value (Min) after normalization are presented in Table 1. Within this local database, only VS exhibits a notable standard deviation of 32.454, attributed to the substantial variation in the data. Conversely, the remaining parameters have relatively small deviations, all less than 5, and do not significantly impact the overall consistency.

Table 1

Statistical analysis of research variables

Variable	Max	Min	Mean	σ
QT	23.490	1.760	6.620	4.096
FS	1.079	0.015	0.227	0.223
BQ	1.004	0.088	0.561	0.188
VS	257.486	86.179	133.862	32.454
OCR	7.652	1.003	2.014	1.084
ST	25.713	1.068	5.168	4.636
SU	0.965	0.113	0.441	0.196

2.2. Method

Bayesian optimization was first applied to the base model, which was to improve the accuracy and generalization of the base model. In addition, to assess the superiority of the KMR model, five base models (KNN, MLP, RF, SVR and XGBoost) are selected as the basis for this study. These five algorithms are also the most commonly used basic algorithmic models for machine learning and are highly applicable [14–18]. Three of these models are arbitrarily selected to construct a stacked model for computational analysis, and the results obtained are compared with those of the target model (the KMR stacked model) to analyse the superiority of the model.

Among them, the Bayesian optimisation algorithm is based on the Bayesian principle to find a kind of functional relationship between the loss function and hyper-parameters [19], which can find the optimal combination of hyper-parameters in the shortest time.

Stacking represents an integrated model framework for hierarchical computation; it is not an algorithm but a high-level integration strategy. Typically, stacking involves a two-level network. Level 0 comprises various base models [20, 21]. Using k-fold cross-validation, predictions are made for the original training dataset. For level 1, the model takes the output of the base models from level 0, along with the original training dataset. The average of the test dataset from the level 0 model is then used for prediction, resulting in the completion of the model.

After dividing the dataset into training and test sets with a 7:3 ratio and normalizing the dataset (Equation 8), the training set is further split into five parts (Train1, Train2, Train3, Train4, Train5). Each part is used as the validation set in turn, while the remaining four parts serve as the training set. The model undergoes training using a 5-fold cross-validation, leading to predictions. This process yields predicted values for all training sets on the base model, with the averages of the five test sets forming the final prediction. Subsequently, the predicted and measured values from different models are utilized as a new training set for further training. The model is then employed to make predictions on this new test set, and the results constitute the final prediction of the stacked model (Fig. 1).

$$x_{nor}=\frac{x-x_{\min}}{x_{\max}-x_{\min}} \tag{8}$$

where x_{nor} is the value of the variable, $x_{\min}$ and $x_{\max}$ are the minimum and maximum values of the variable, respectively.

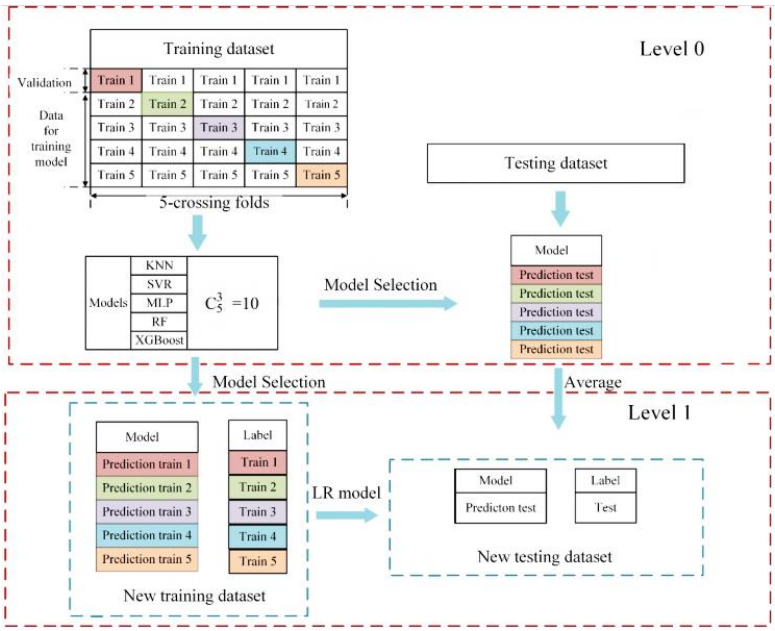

Fig 1 – Schematic diagram of the stacked model calculation.

2.3. Evaluation indicators

RMSE, R^2 and MAPE error indicators are used to assess the strengths and weaknesses of the model's computational results. The RMSE reflects the difference between the measured data and the predicted data. R^2 reflects the overall fit of the model curve, with a value closer to 1 indicating a better fit. Given the small variability in the SU range (0–1.2), MAPE is particularly effective in assessing the error between measured and predicted values. The calculation formula for the evaluation indices is as follows:

$$\mathrm{RMSE} = \sqrt{\frac{1}{n}\sum_{i=1}^{n}(\hat{y}_i - y_i)^2} \tag{9}$$

$$\mathrm{MAPE} = \frac{100}{n}\sum_{i=1}^{n}\left|\frac{\hat{y}_i - y_i}{y_i}\right| \quad [\%] \tag{10}$$

$$R^2 = 1 - \frac{\sum_{i=1}^{n}(\hat{y}_i - y_i)^2}{\sum_{i=1}^{n}(\bar{y}_i - y_i)^2} \tag{11}$$

where $\hat{y}_i$ and y_i respectively represent the predicted values and true values on the test set, and $\bar{y}$ is the average value.

3. RESULTS AND DISCUSSION

3.1. Bayesian optimization results

The Bayesian optimization calculations were executed in the Python language environment utilizing the hyperopt library. The optimization metric was analyzed using the RMSE, commonly employed in regression algorithms (Eq. 11). The number of iterations for the model was set to 1000, and the results are presented in Table 2.

Table 2

The result of hyperparametric

Models	hyper-parameter (optimal value)
KNN	n_neighbors (5)
SVR	C (3.379); epsilon (0.123); gamma (0.001)
MLP	hidden_layer_sizes (128,64,64); max_iter (20000)
RF	max_depth (18); max_features (2); min_samples_leaf (2);min_samples_split (7); n_estimators (47)
XGBoost	n_estimators (393); learning_rate (0.029); in_child_weight (15);max_depth (14); subsample (0.864); colsample_bytree (0.805);gamma (1); reg_alpha (0.101); reg_lambda (0.104)

Individually, the RF and XGBoost models outperformed KNN, SVR, and MLP significantly. The model's RMSE ranged from 0.089 to 0.112, R^2 ranged from 0.513 to 0.658, and MAPE ranged from 21.40 to 29.55 (Fig. 2). Overall, the model exhibited improved performance following hyperparameter optimization.

Specifically, it is evident that the KNN model is more accurate in predicting SU within the range of 0–0.65, the SVR model excels in predicting SU within the range of 0.2–0.65, the XGBoost model demonstrates higher accuracy in predicting SU within the range of 0 – 0.70, MLP proves to be more accurate in predicting SU within the range of 0.2 – 0.8, and the RF model exhibits greater accuracy in predicting SU within the range of 0.2 – 0.6. The optimized values resulted in enhanced accuracy across the board.

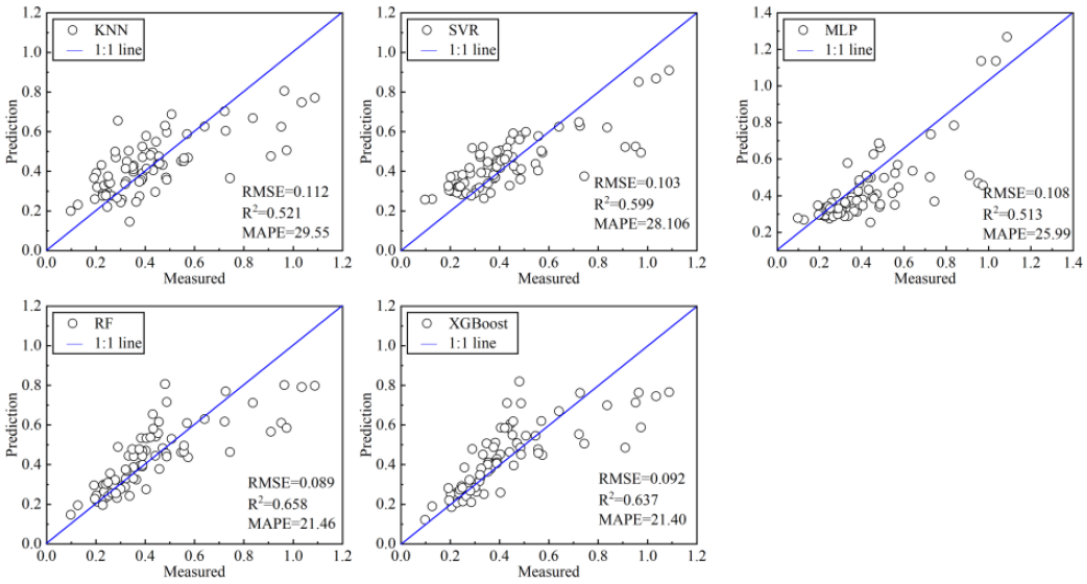

Fig. 2 – The test results of base models after optimization.

3.2. Results of the stacked model

After subjecting the foundational model to the stacked model process, we derived prediction accuracies for all stacked models on the test set, as illustrated in Fig. 3. The root mean square errors (RMSE) for the three stacked models range from 0.0852 to 0.101, the *R*-squared (R^2) values range from 0.571 to 0.702, and the mean absolute percentage errors (MAPE) range from 19.68 to 26.5. Upon analyzing the results, it is evident that the accuracies of the three stacked models surpass those of individual models, signifying a notable enhancement in overall model accuracy. This substantiates the efficacy of stacked models in effectively amalgamating the strengths of base models.

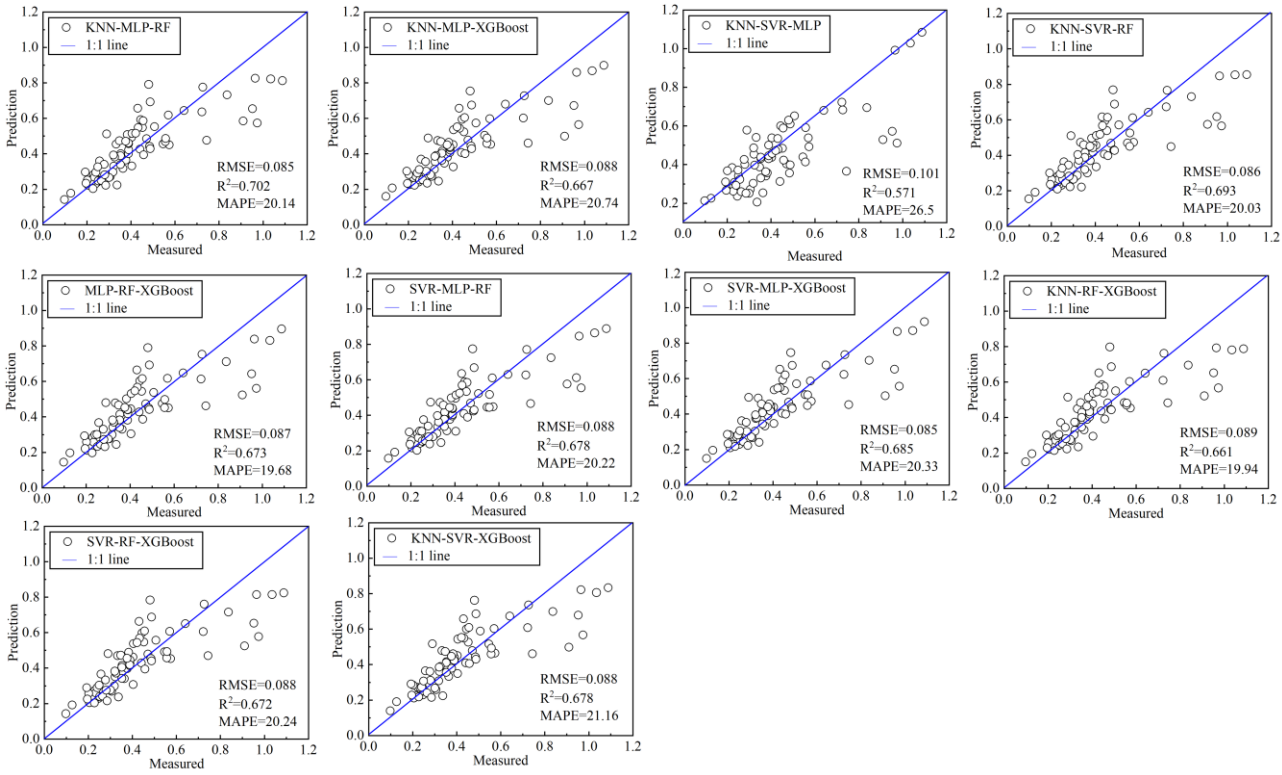

Fig. 3 – Stack model prediction results on test set.

Furthermore, Fig. 3 indicates that K-nearest neighbors (KNN) plays a pivotal role in elevating model prediction accuracy, outperforming support vector regression (SVR). Particularly, when KNN is integrated with multilayer perceptron (MLP) and random forest (RF) models, there is a significant enhancement in model accuracy. Additionally, a comparison of stacked models involving RF and XGBoost, the two mainstream integrated models, reveals that the KNN-MLP-RF model outshines all other combinations. This underscores the superior predictive accuracy of the KNN-MLP-RF stacked model, showcasing its adept integration of each model's advantages and emphasizing its substantial superiority in prediction accuracy.

3.3. Comparative analysis of stacked models and empirical formulations

Undrained shear strength was estimated using empirical equations proposed by Robertson *et al.* (2020), Senneset *et al.* (1985) and Jamiolkowski *et al.* (1985) [22–24]. These formulae were adapted to suit the SU calculations, resulting in equations 12 to 14:

$$\mathrm{SU} = s_u/\sigma'_{vo} = \frac{(q_t - \sigma_{vo})/\sigma'_{vo}}{N_{kT}} \tag{12}$$

$$\mathrm{SU} = s_u/\sigma'_{vo} = \frac{(q_t - u_2)/\sigma'_{vo}}{N_{kE}} \tag{13}$$

$$\mathrm{SU} = s_u/\sigma'_{vo} = (0.23 \pm 0.04)(\mathrm{OCR}^{0.8}) \tag{14}$$

The total cone tip coefficient N_{kT} has a range of 11 to 19, while the effective cone tip coefficient N_{kE} ranges from 6 to 12. QT, defined in this paper as $(q_t - \sigma_{vo})/\sigma'_{vo}$. However, formula (13) is derived based on normally consolidated soil, and in this study, the OCR is consistently greater than 1, indicating overconsolidated soil. Therefore, for calculations, formula (12) and formula (14) are selected.

As N_{kT} is an empirical parameter, an optimization algorithm is employed to determine its value, with RMSE as the regression optimization criterion. After calculations, when N_{kT} equals 16, formula (12) exhibits the best predictive accuracy, yielding an RMSE of 0.111 (Fig. 4a). According to formula (14), SU shows a

linear relationship with OCR 0.8. To determine the optimal coefficient value, we analyze the end values of (0.23±0.04). Upon calculation, when the coefficient is set to 0.27, the RMSE is 0.101. When the coefficient is 0.19, the RMSE is 0.128. Since a smaller RMSE indicates better predictive accuracy, the coefficient of 0.27 is chosen.

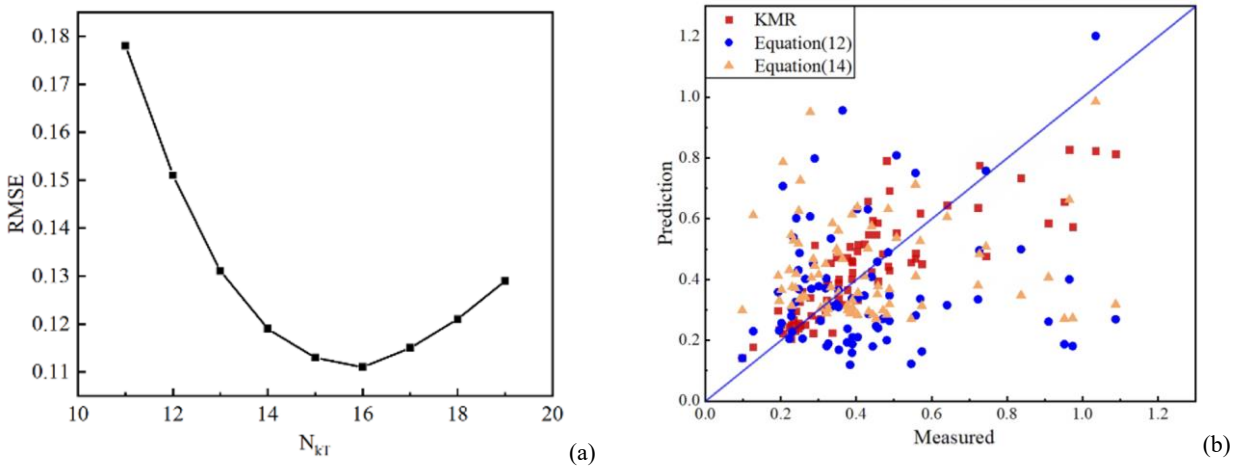

(a) (b)

Fig. 4 – Analysis of empirical equations results: (a) Intelligent optimization results for N_{kT}; (b) Prediction results of empirical formula and KMR model.

Comparing the predicted results with empirical formulas (Fig. 4b), it is observed that the accuracy of the KMR model far exceeds that of the empirical formulas. Results from formula (14) slightly outperform those of formula (12), indicating that OCR has a greater impact on undrained shear strength. When SU values range from 0.6 to 1.2, the calculated values from the empirical formula deviate significantly, suggesting its inapplicability in predicting SU under these conditions.

Therefore, in situations where empirical formulas are not applicable, employing the KMR (KNN-MLP-RF) model provides a better prediction of the undrained shear strength of clay, ensuring the accuracy of various parameters during engineering implementation.

3.4. Parameters importance analysis

In soil mechanics, it is well-understood that the undrained shear strength (Su) of soil is influenced by several key parameters, including cone tip resistance QT, pore water pressure, and overconsolidation ratio (OCR). These factors are closely related to the soil's stress history, consolidation state, and effective stress conditions, which directly impact its strength and deformation characteristics. For instance, OCR is a crucial factor as it reflects the soil's previous loading history, where a higher OCR typically indicates a soil that has been pre-consolidated to a greater stress than it currently experiences, leading to higher shear strength. Similarly, QT, measured from cone penetration tests, is an indicator of the soil's resistance to penetration, which correlates with its stiffness and shear strength. Pore pressure plays a significant role in effective stress and, consequently, in determining Su, especially in undrained conditions where changes in pore pressure can lead to variations in soil strength.

To quantify the influence of these parameters, we conducted a feature importance analysis using the Random Forest (RF) model's feature importances attribute and Spearman's correlation coefficient (r_s). The RF model, implemented via Python, provided a ranking of parameters based on their relative importance to Su, while (r_s) was used to assess the correlation between pairs of variables, calculated using equation as follow [25]:

$$r_s = 1 - \frac{6\sum(x_i - y_i)^2}{n(n^2 - 1)} \tag{15}$$

The results consistently showed that OCR has the greatest impact on Su, followed by QT, side friction resistance, shear wave velocity, and pore pressure parameter. This ranking is consistent with soil mechanics

principles, where OCR's dominance is expected due to its direct relationship with the soil's pre-consolidation and stress history, which governs the stiffness and strength of the soil. The significant influence of QT is also anticipated, as it reflects the overall soil resistance, which correlates with shear strength. FS, representing side friction during penetration testing, and VS, indicating soil stiffness through shear wave propagation, further contribute to understanding the soil's shear strength. The relatively lower influence of BQ aligns with its more indirect relationship to Su.

Although the exact numerical values of feature importance differ between the RF model and Spearman's correlation analysis, the consistent trend observed in the rankings validates the robustness of our approach. Moreover, these findings are supported by empirical equations commonly used in geotechnical engineering, demonstrating that our model not only performs well mathematically but is also firmly grounded in soil mechanics theory. By integrating these principles into our analysis, we ensure that the results are both scientifically sound and practically applicable.

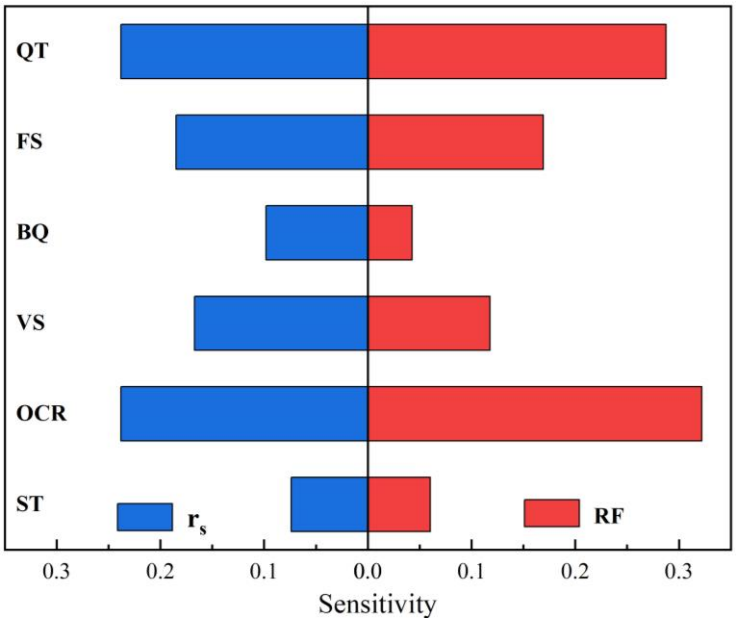

Fig. 5 – Sensitivity for different parameters.

4. CONCLUSION

This paper introduces a method based on the KMR stacking model to enhance the prediction accuracy of undrained shear strength for clay. Through a comprehensive comparative analysis of the strengths and weaknesses of the base model, stacking model, and empirical formulas.

In the comparative analysis between stacking models and single base models, the stacking models successfully integrate the advantages of the base models, resulting in improved calculation accuracy. However, the degree of improvement in calculation accuracy varies for different models, with the minimum increase being only 1.5%. In contrast, the KMR model more effectively integrates the algorithmic strengths of each model, achieving higher accuracy and a maximum improvement of 18.9%.

Comparisons between stacking models and empirical formulas in calculation results indicate that the KMR stacking model provides more accurate predictions of undrained shear strength. Moreover, even in cases where SU values are relatively high and the calculated values from empirical formulas deviate significantly, this method still delivers relatively accurate results, demonstrating the robustness of the model.

Therefore, the KMR stacking algorithm not only enhances the prediction accuracy of undrained shear strength but also provides a reference for feature selection in predicting soil parameters. This holds significant reference value and importance for the safe implementation of work in geotechnical engineering and related fields.

ACKNOWLEDGMENTS

The authors would like to acknowledge the grant 20210302124438 support by by Shanxi province, China. The authors are very grateful to the academics involved for making the data publicly available in the study.

REFERENCE

[1] Krabbenhøft K, Galindo-Torres SA, Zhang X, Krabbenhøft J. AUS: Anisotropic undrained shear strength model for clays. International Journal for Numerical and Analytical Methods in Geomechanics. 2019; 43(17): 2652–2666.

[2] Li X, Zhang L, Xiao T, Zhang S, Chen C. Learning failure modes of soil slopes using monitoring data. Probabilistic Engineering Mechanics. 2019; 56: 50–57.

[3] Kang X, Sun HM, Luo H, Dai T, Chen RP. A portable bender element-double cone penetration testing equipment for measuring stiffness and shear strength of in-situ soft soil deposits. KSCE Journal of Civil Engineering. 2020; 24(12): 3546–3560.

[4] Ching J, Phoon K-K. Constructing site-specific multivariate probability distribution model using Bayesian machine learning. Journal of Engineering Mechanics. 2019; 145(1): 04018126.

[5] Larsson R, Åhnberg H. On the evaluation of undrained shear strength and preconsolidation pressure from common field tests in clay. Canadian Geotechnical Journal. 2005; 42(4): 1221–1231.

[6] Cai G, Liu S, Tong L, Du G. Assessment of direct CPT and CPTU methods for predicting the ultimate bearing capacity of single piles. Engineering Geology. 2009; 104(3–4): 211–222.

[7] Duan W, Cai G, Zou H, Liu S. 2018. Evaluation of liquefaction potential of saturated sands based on resistivity piezocone penetration testing – A case study. In: Bian X, Chen Y, Ye X, editors. Environmental Vibrations and Transportation Geodynamics. Singapore; 2016. Springer, pp. 509–514.

[8] Asghari V, Leung YF, Hsu SC. Deep neural network based framework for complex correlations in engineering metrics. Advanced Engineering Informatics. 2020; 44: 101058.

[9] Mbarak WK, Cinicioglu EN, Cinicioglu O. SPT based determination of undrained shear strength: Regression models and machine learning. Frontiers of Structural and Civil Engineering. 2020; 14(1): 185–98.

[10] Pham BT, Prakash I, Singh SK, Shirzadi A, Shahabi H, Tran TTT, Bui DT. Landslide susceptibility modeling using Reduced Error Pruning Trees and different ensemble techniques: Hybrid machine learning approaches. Catena. 2019; 175: 203–218.

[11] Wang T, Zhang K, Thé J, Yu H. Accurate prediction of band gap of materials using stacking machine learning model. Computational Materials Science. 2022; 201: 110899.

[12] Zou H, Liu S, Cai G, Puppala AJ, Bheemasetti TV. Multivariate correlation analysis of seismic piezocone penetration (SCPTU) parameters and design properties of Jiangsu quaternary cohesive soils. Engineering Geology. 2017; 228: 11–38.

[13] Wroth CP. The interpretation of in situ soil test. Géotechnique. 1984; 34(4): 449–489.

[14] Kardani MN, Baghban A. Utilization of LSSVM strategy to predict water content of sweet natural gas. Petroleum Science and Technology. 2017; 35(8): 761–767.

[15] Garcia S, Derrac J, Cano JR, Herrera F. Prototype selection for nearest neighbor classification: Taxonomy and empirical study. IEEE Transactions on Pattern Analysis and Machine Intelligence. 2012; 34(3): 417–35.

[16] Jin Z, Shang J, Zhu Q, Ling C, Xie W, Qiang B. RFRSF: Employee turnover prediction based on random forests and survival analysis. In: Huang Z, Beek W, Wang H, Zhou R, Zhang Y, editors. Web Information Systems Engineering – WISE 2020. Lecture Notes in Computer Science, vol. 12343. Cham: Springer; 2020, pp. 503–515.

[17] Youssef AM, Pourghasemi HR, Pourtaghi ZS, Al-Katheeri MM. Erratum to: Landslide susceptibility mapping using random forest, boosted regression tree, classification and regression tree, and general linear models and comparison of their performance at Wadi Tayyah Basin, Asir Region, Saudi Arabia. Landslides. 2016; 13(5): 1315–1318.

[18] Li X, Ran Z, Zheng D, Hu C, Qin Z, Wang H, Wang Z, Li P. Dynamic bond stress-slip relationship of steel reinforcing bars in concrete based on XGBoost algorithm. Journal of Building Engineering. 2024; 84: 108368.

[19] Zhang Q, Hu W, Liu Z, Tan J. TBM performance prediction with Bayesian optimization and automated machine learning. Tunnelling and Underground Space Technology. 2020; 103: 103493.

[20] Dou J, Yunus AP, Bui DT, Merghadi A, Sahana M, Zhu Z, Chen C-W, Han Z, Pham BT. Improved landslide assessment using support vector machine with bagging, boosting, and stacking ensemble machine learning framework in a mountainous watershed, Japan. Landslides. 2020; 17(3): 641–658.

[21] Ribeiro MHDM, Dos Santos Coelho L. Ensemble approach based on bagging, boosting and stacking for short-term prediction in agribusiness time series. Applied Soft Computing Journal. 2020; 86: 105837.

[22] Robertson PK, Campanella RG, Gillespie D, Greig J. Use of piezometer cone data. Engineering, Geology, Environmental Science. 1986: 1263–1280.

[23] Jamiolkowski M, Ladd CC, Germaine JT, Lancellotta R. New developments in field and laboratory testing of soils. In: Proceedings of the 11th International Conference on Soil Mechanics and Foundation Engineering. San Francisco; 1985.

[24] Senneset K, Janbu N. Shear strength parameters obtained from static cone penetration tests. Philadelphia, PA: ASTM Special Technical Publication; 1985, pp. 41–54.

[25] Zar JH. Significance testing of the Spearman rank correlation coefficient. Journal of the American Statistical Association. 1972; 67(339): 578–580. https://doi.org/10.1080/01621459.1972.10481251.

Received March 14, 2024